Cell

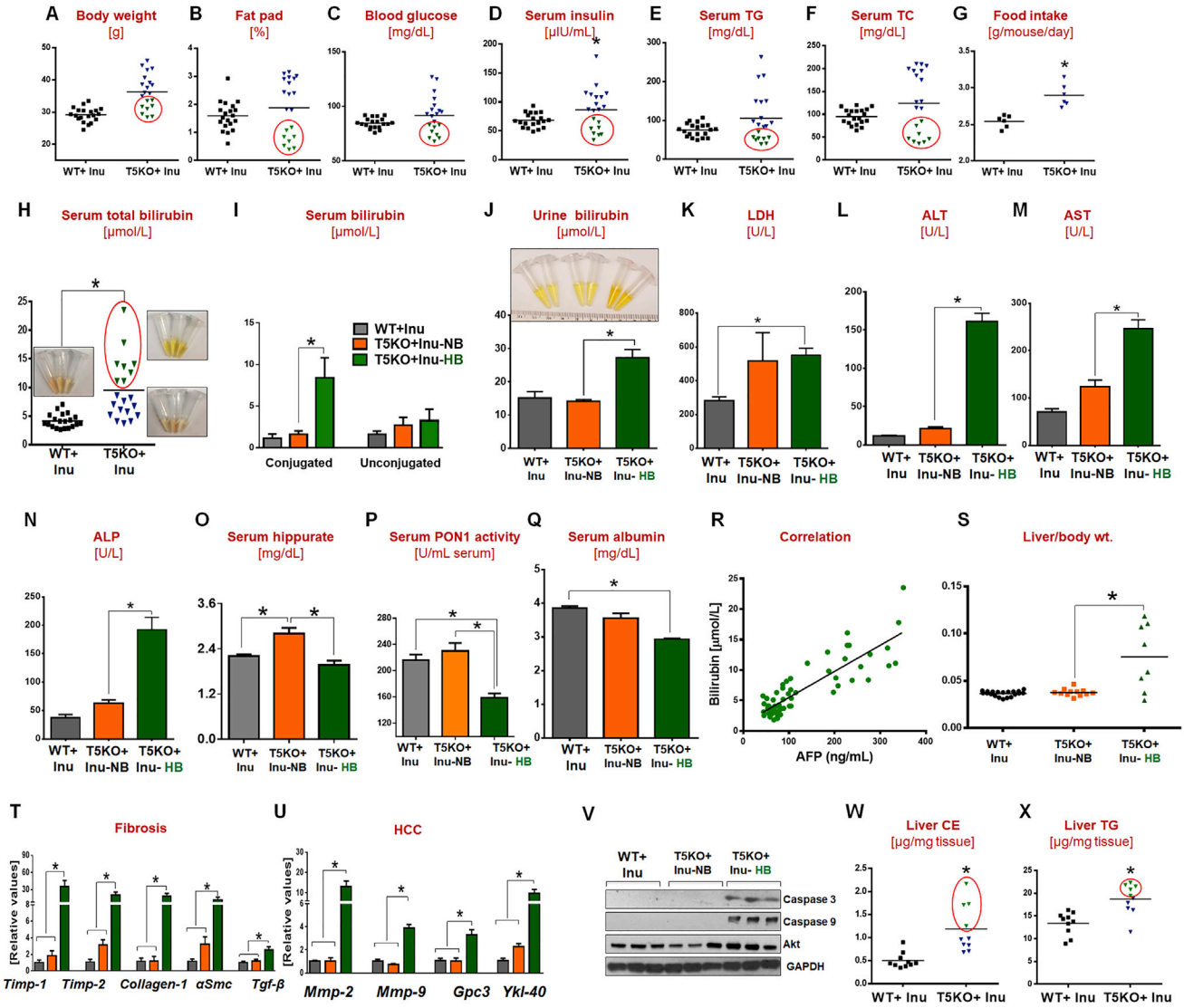

Figure S1. Dietary Inulin (Polyfructosan) Protects against Indices of Metabolic Syndrome but Induces Liver Dysfunction in a Subset of TLR5-Deficient Mice, Related to Figure 1

Four-week-old male *T5*KO mice and WT controls (n = 20) were fed ICD for 24 weeks. Mice were monitored for body weight (weekly) and food intake monthly. Hemolysis-free serum was subjected to metabolic parameters.

(A–C) (A) Body weight, (B) fat pad, and (C) 15h fasting blood glucose.

(D–F) Fasting (5h) serum concentrations of: (D) insulin, (E) triglycerides (TG), and (F) total cholesterol (TC).

(G–I) Dot plot represents food intake; each point represents average food consumed by group of 10 mice. Additionally, serum samples were analyzed for (H) total bilirubin (image illustrates the yellow tinge due to bilirubin accumulation in sera from *T5*KO+Inu-HB, but not in WT+Inu and *T5*KO+Inu-NB), and (I) conjugated and unconjugated bilirubin.

(J) Image (upper panel) and bar graph (lower panel) represent total bilirubin in urine.

(K–Q) Serum levels of (K) lactate dehydrogenase (LDH), (L) ALT, (M) AST, (N) alkaline phosphatase (ALP), (O) hippurate, (P) serum paraoxonase 1 (PON1) activity, and (Q) albumin.

(R) Mice with normal and high bilirubin were analyzed for correlation between serum bilirubin and AFP [Pearson correlation coefficient r = 0.86, p (two-tailed) < 0.0001].

(S) Liver to body weight ratio.

(T and U) Bar graph depicts the relative gene expression of hepatic (T) fibrosis (*Timp-1, Timp-2, Collagen-1, αSmc, Tgf-β*), and (U) HCC markers (*Mmp-2, Mmp-9, GPC3, Ykl40*).

(V–X) Immunoblot showing liver caspase 3, caspase 9 and Akt. Dot plots represent hepatic (W) cholesteryl ester (CE), and (X) triglycerides (TG) in ICD-fed mice. Red circle delineates values from *T5*KO+Inu-HB mice. Each dot represents the data from one mouse. The data are representative of two independent experiments. (*p < 0.05).

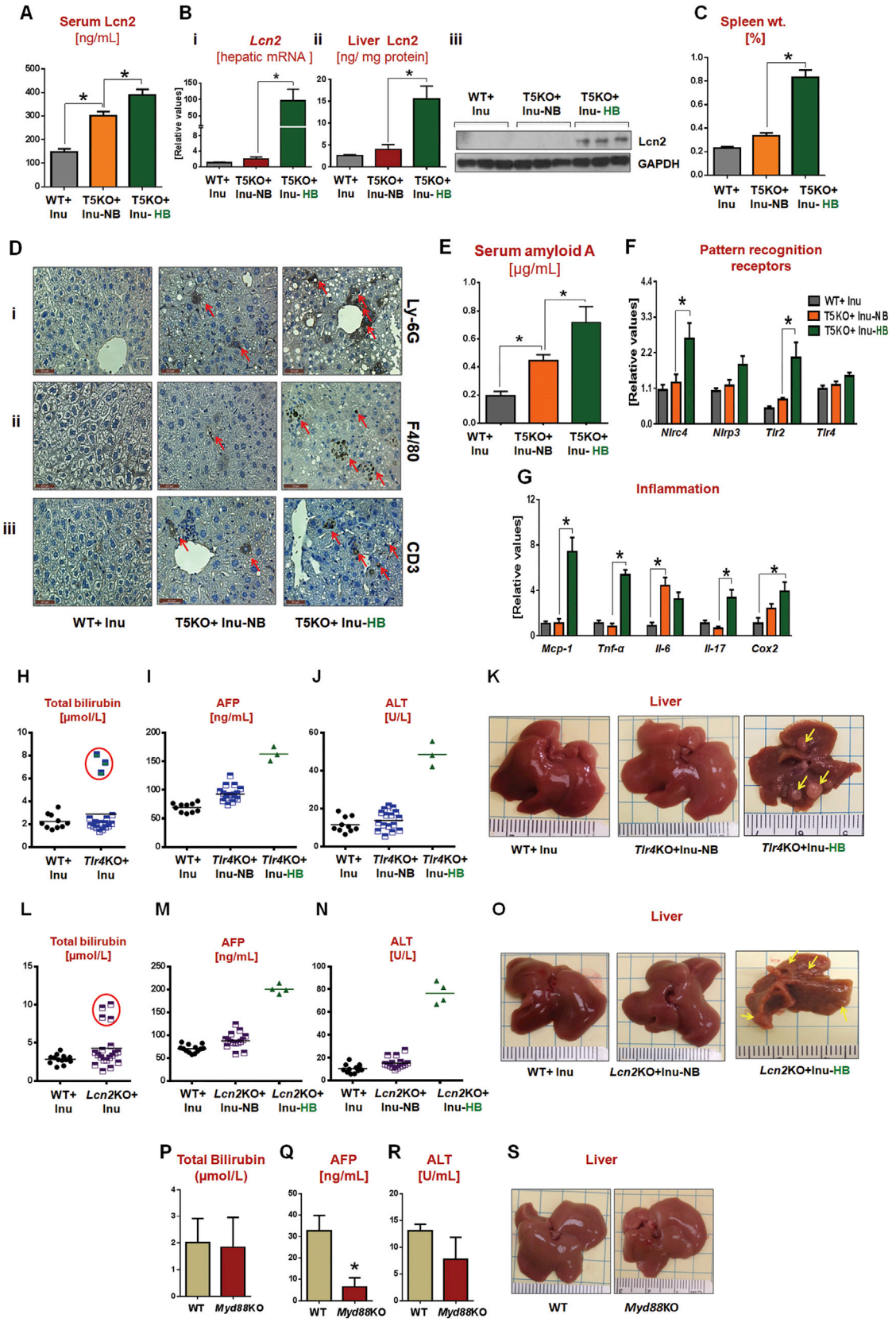

(legend on next page)

Figure S2. ICD-Fed TLR5-Deficient Mice Exhibit Hepatic and Low Grade Systemic Inflammation, Related to Figure 1

Four-week-old male *T5*KO mice and WT control (n = 20) were fed ICD for 6 months.

(A) Bar graph displays serum Lcn2.

(B) Liver samples from ICD-fed mice were analyzed for Lcn2 at (i) mRNA, and protein level through (ii) ELISA, and (iii) Western blotting.

(C) Percent spleen weight.

(D) Images show the immunostaining of (i) Ly-6G, marker for neutrophils, (ii) F4/80, marker for macrophages, and (iii) CD3, a pan T cell marker in the liver samples obtained from ICD-fed WT and *T5*KO mice (scale bar = 20 μm). Red arrows highlight the indicated immune cells.

(E) Serum level of serum amyloid A.

(F and G), Bar graph represents quantitative expression of (F) hepatic pattern recognition receptors (*Nlrc4, Nlrp3, Tlr2 and Tlr4*), and (G) liver pro-inflammatory genes (*Mcp-1, Tnf-α Il-6, Il-17 and Cox2*). The data are representative of 2 independent experiments.

(H–K) Four weeks old WT (n = 10) and *T4*KO (n = 18) mice fed with ICD for 6 months. Dot plots represent the serum level of (H) total bilirubin, (I) AFP, and (J) alanine aminotransferase (ALT). (K) Image display the gross liver phenotype.

(L–O) Similarly, WT (n = 13) and *Lcn2*KO (n = 19) mice were fed with ICD and examined for (L) serum total bilirubin, (M) AFP, (N) ALT, and (O) gross liver phenotype.

(P–S) In a separate set of experiment, four weeks old male *Myd88*KO and WT control (n = 10) were fed on ICD for 6 months. Bar graphs show the serum concentration of (P) total bilirubin, (Q) AFP, and (R) ALT. (S) Image display the gross liver appearance. Each dot represents the data from one mouse. The values expressed as mean ± SEM (*$p < 0.05$).

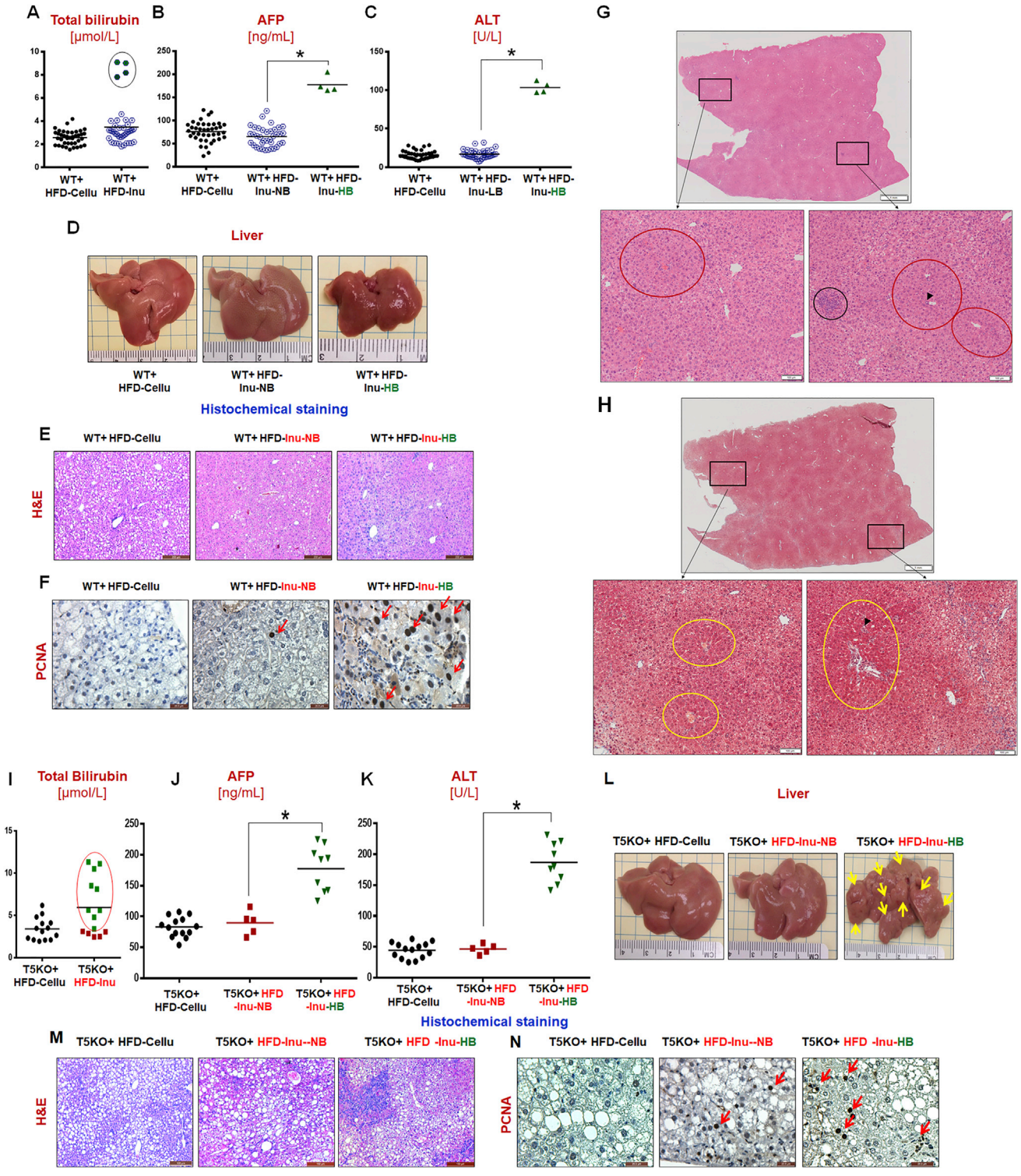

Figure S3. High Fat Diet Enriched with Inulin Induces HCC in WT and Aggravates HCC in TLR5-Deficient Mice, Related to Figure 1

Four-week-old male WT mice (n = 41) were fed a high-fat diet supplemented with cellulose or inulin for 6 months and analyzed for hallmark parameters related to HCC.

(A–C) Dot plot represents serum level of (A) total bilirubin, (B) AFP, and (C) ALT.

(D–F) Image display the (D) gross pictures of liver (incidence of HCC: ~10%), (E) H&E stained [scale bar (SB) = 200 μm] liver, and (F) immunostaining for PCNA (SB = 20 μm).

(legend continued on next page)

(G and H) (G) H&E-stained and (H) Masson's trichrome-stained liver section; the boxed region in the top image is further magnified in the bottom panel [SB = 1 mm (upper panle) and 100 μm (lower panel)]. Red and yellow circles denote small well-differentiated tumor with trabecular pattern. Small black circle in the lower left panel (G) shows inflammatory foci. Black arrowhead indicates the bile duct. Collagen fibers appeared as blue colored stain in lower right panel (H). Four weeks old male *T5*KO were maintained on either cellulose or inulin supplemented with high fat and examined for HCC markers.

(I–K) Dot plot display the serum (I) total bilirubin, (J) AFP and (K) ALT.

(L–N) Image show the (L) gross liver appearance (incidence of HCC: ~65%), (M) H&E-stained liver (SB = 100 μm), and (N) PCNA immunostaining (SB = 20 μm). Yellow arrows highlight the tumor nodules. Red arrows point the PCNA positive cells. Each dot represents the data from one mouse. (*$p < 0.05$).

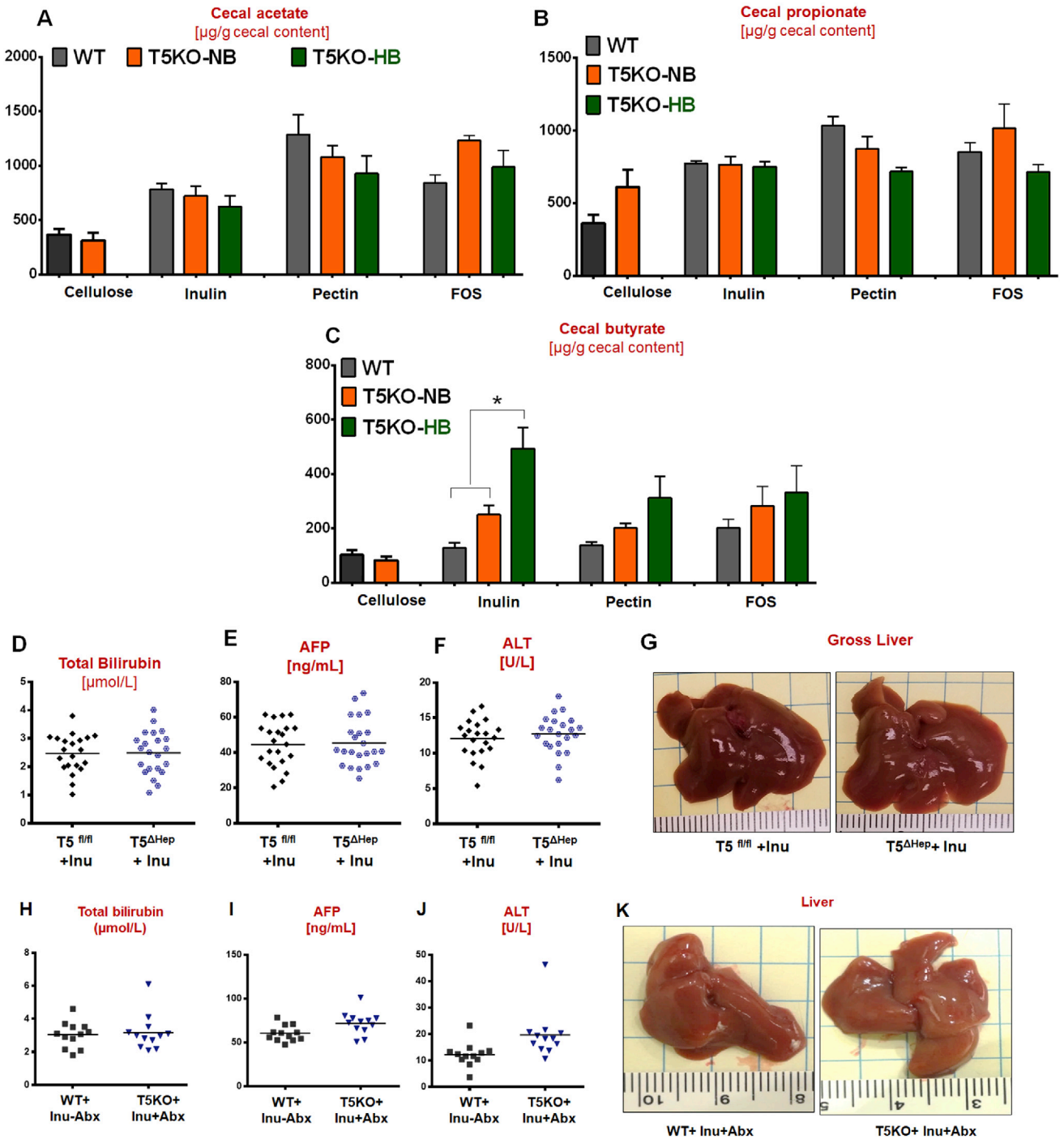

(figure continued on next page)

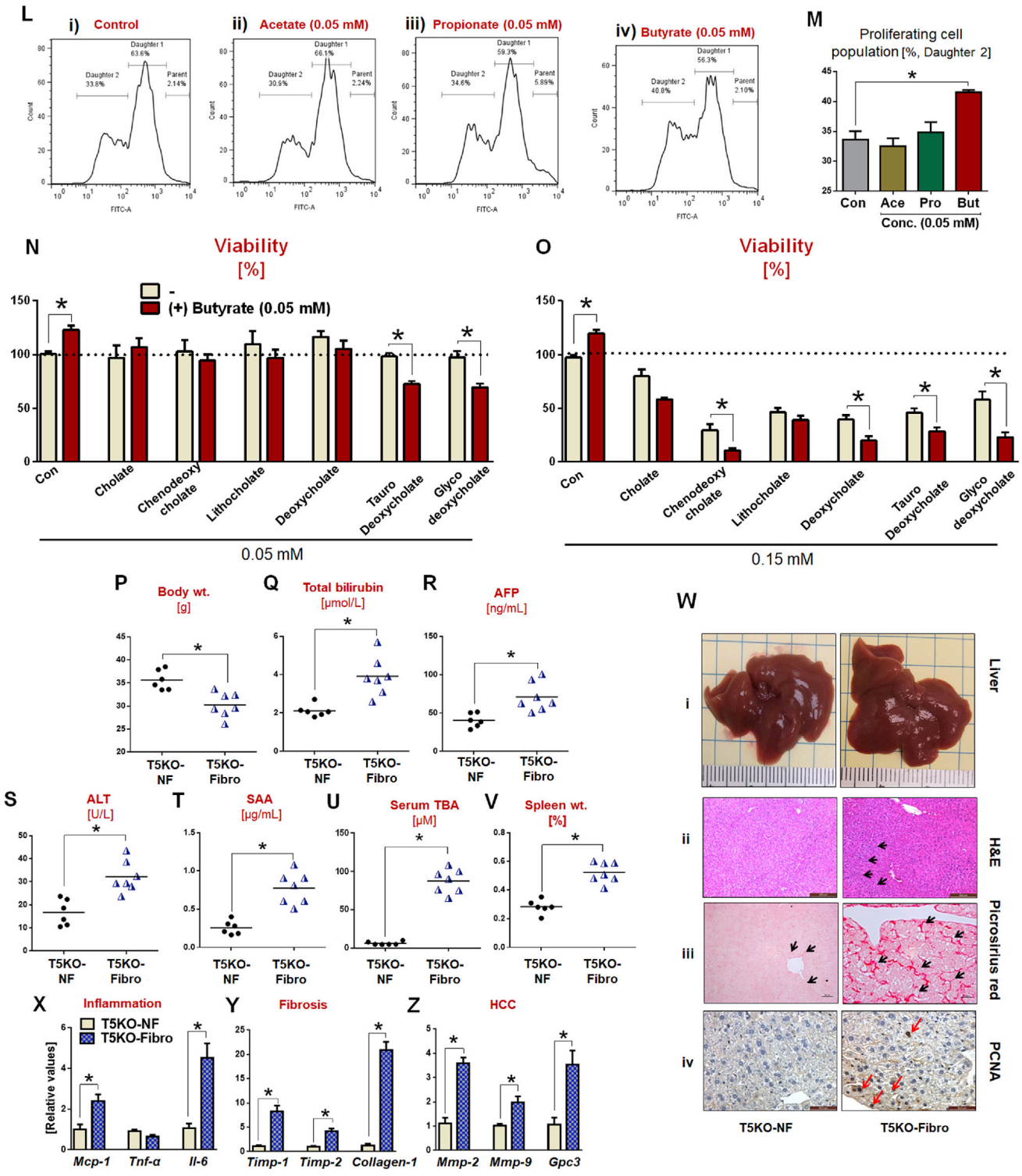

Figure S4. Altered Gut Microbiota-Generated Products Mediate HCC Pathogenesis in Dietary Soluble Fiber fed *T5*KO Mice, Related to Figure 3

Four-week-old male *T5*KO mice and WT controls were fed CCD, ICD, or PCD for 24 weeks. After euthanasia, SCFA were measured in cecal contents using GC-MS.

(legend continued on next page)

(A–C) Bar graph depicts relative abundance of (A) acetate (B) propionate, and (C) butyrate in cecal contents. In a separate set of experiment, four weeks old *Tlr5*$^{fl/fl}$ and *Tlr5*$^{\Delta Hep}$ mice (n = 21-22) were fed on ICD for 6 months. At the time of euthanasia, mice were bled retro-orbitally and screened for serum bilirubin and other markers of hepatic damage including gross livers.

(D–G) (D) Serum bilirubin, (E) AFP, (F) ALT, (G) gross liver. In another set of experiment ICD-fed WT and *T5*KO (n = 12) were simultaneously administered with broad spectrum antibiotic (ampicillin and neomycin 1.0 and 0.5 g/L respectively) in drinking water for 6 months.

(H–K) Dot plot depicts the serum level of (H) total bilirubin, (I) AFP, (J) ALT, and K) Images show the gross liver. Hepa-1c1c7 mouse hepatocytes cell line were treated with 5.0 μM carboxyfluorescein succinimidyl ester (CFSE) and seeded in 24 well plate in αMEM media. Cells were stimulated with acetate, propionate and butyrate (0.05 mM) for 72h and proliferating cell population was analyzed via flow cytometer.

(L) Histogram represents the cell proliferation pattern in (i) control, (ii) acetate, (iii) propionate, and (iv) butyrate treated cells.

(M) Bar graph represents the percent proliferative cell population present in Daughter 2 segment of histogram.

(N and O) Hepa-1c1c7 mouse hepatocytes were pre-incubated with butyrate (0.05 mM) containing media for 24 h and then treated with different bile acids (0.05 mM for another 24 h) as indicated in the figure. Similarly, in another set of experiment, butyrate (0.05 mM) pretreated hepatocytes were challenged with 3-fold more (0.15 mM) concentrated bile acids. Cell viability was assessed by MTS assay. (N and O) Bar graphs represent percent (%) viability of hepatocytes in presence of different bile acids. P-Z) In another set of experiment, four weeks old *T5*KO mice (male, n = 13) were fed with sodium butyrate (100 mM) in drinking water for 36 weeks. Control mice received sodium-matched drinking water.

(P) Body weight of *T5*KO mice with no hepatic fibrosis (*T5*KO-NF) and *T5*KO mice with hepatic fibrosis (*T5*KO-Fibro).

(Q–V) Dot plot represents the serum (Q) total bilirubin, (R) AFP, (S) ALT, and (T) serum amyloid A (SAA, a clinical marker of active inflammation), (U) total bile acid (TBA). (V) Dot plot shows percent spleen weight. Each dot represents the data from one mouse.

(W) Images display (i) gross liver, (ii) H&E stained liver sections [scale bare (SB) = 200 μm; arrows highlighting infiltrated cells), (iii) picrosirius red staining (SB = 50 μm), and (iv) PCNA immunostaining (SB = 50 μm) which depicts an increase in proliferating hepatocytes (red arrow) was observed in *T5*KO-Fibro compared to *T5*KO-NF.

(X–Z) Bar graph represents the relative expression of markers of hepatic (X) inflammation (*Mcp-1*, *Tnf-α*, *Il-6*), (Y) fibrosis (*Timp-1*, *Timp-2*, *Collagen-1*), and (Z) HCC (*Mmp-2*, *Mmp-9*, *Gpc3*). Values are expressed as mean ± SEM (*p < 0.05).

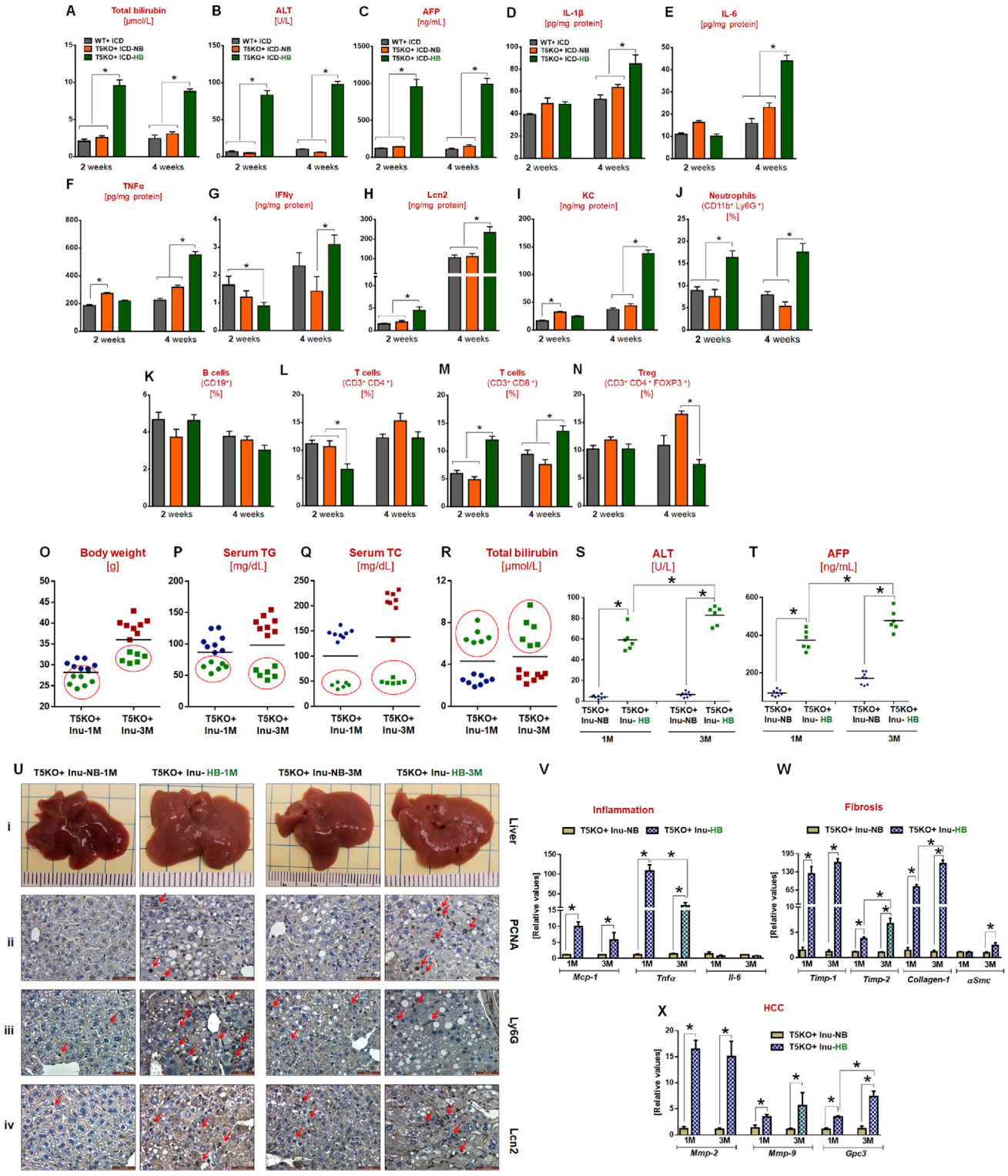

(figure continued on next page)

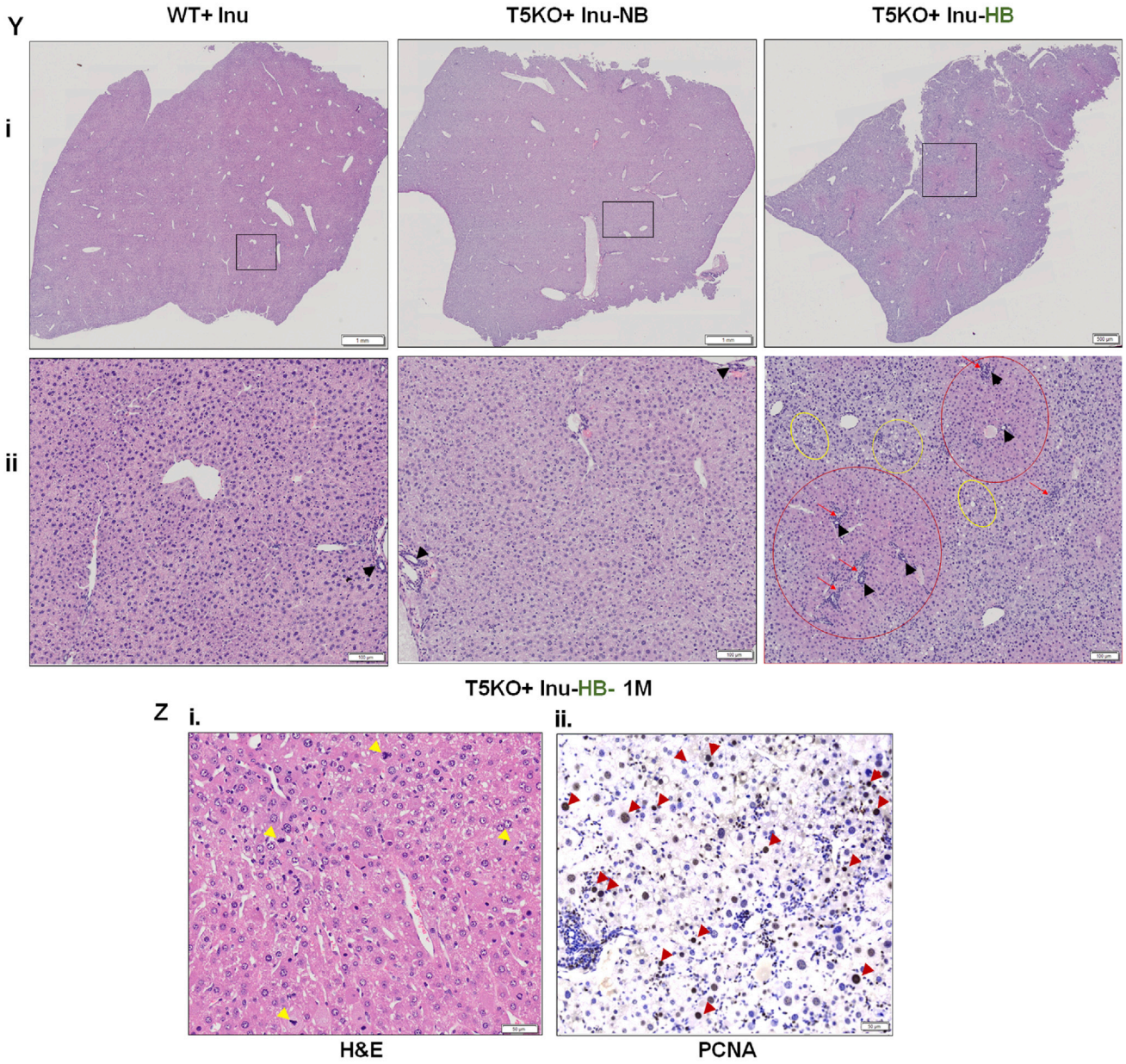

Figure S5. Early Signs of Hepatic Inflammation and HCC Development in Short-Term ICD-Fed Hyperbilirubinemic *T5*KO Mice, Related to Figure 7

(A–C) Four-week-old male *T5*KO mice and their WT littermates (n = 5-14) were fed on ICD for 2 and 4 weeks. At indicated time points, mice were bled retroorbitally, screened for serum bilirubin and segregated into N-bili and H-bili *T5*KO mice and analyzed for liver for pro-inflammatory cytokines and immune cell composition. Bar graphs represent serum level of (A) bilirubin, (B) ALT, and (C) AFP.

(D–I) hepatic level of (D) IL-1β, (E) IL-6, (F) TNFα, (G) IFNγ, (H) Lcn2, and (I) KC (keratinocyte-derived chemokine).

(J–N) Data show the percentage of immune cells in liver (J) Neutrophils, (K) B cells, (L) $CD4^+$T cells, (M) $CD8^+$ T cells and (N) regulatory T cells. To ascertain the time dependent HCC pathogenesis, male *T5*KO mice (n = 14) were maintained on ICD. Serum and liver from normal and high bilirubin mice were analyzed at 1 and 3 months.

(O–T) Dot plots represent (O) body weight, and serum levels of (P) TG, (Q) TC, (R) total bilirubin, red circle delineates values from *T5*KO+Inu-HB mice, (S) ALT, and (T) AFP.

(U) Images display (i) gross liver, and immune staining for (ii) PCNA [scale bar (SB) = 50 μm], (iii) neutrophil (Ly6G, SB = 50 μm), and (iv) Lcn2 (red arrows indicate positively-stained cells, SB = 50 μm). No tumor nodule was observed in the livers from *T5*KO+Inu-HB and *T5*KO+Inu-NB at 1-month and 3-months, although *T5*KO+Inu-HB liver display an increase in hepatocytes proliferation compared to *T5*KO+Inu-NB liver.

(V–X) Quantitative gene expression of hepatic (V) Inflammation (*Mcp-1*, *Tnf-α*, *Il-6*), (W) Fibrosis (*Timp-1*, *Timp-2*, *Collagen-1*, *αSmc*), and (X) HCC (*Mmp-2*, *Mmp-9*, *Gpc3*) markers. Each dot represents the data from one mouse.

(legend continued on next page)

(Y) Representative H&E-stained liver images from WT, *T5*KO-NB, and *T5*KO-HB mice fed ICD for one month [SB = 1 mm (upper panel) and 100 μm (lower panel)]. The boxed regions in the top panel are further magnified in the bottom panel. The hyperbilirubinemic *T5*KO mice showed abnormal features, including cell swelling (red circle), extensive infiltration of immune cells (red arrows) and lipid accumulation (yellow circles). Black arrowhead denotes the bile duct.

(Z) Image show the (i) H&E-stained (SB = 50 μm) and (ii) PCNA-immunostained image (SB = 50 μm) from hyperbilirubinemic *T5*KO mice maintained on ICD for 1 month. Yellow arrowheads denote the mitotic figures. Red arrowheads symbolize the PCNA-positive cells. Values are expressed in mean ± SEM (*$p < 0.05$).

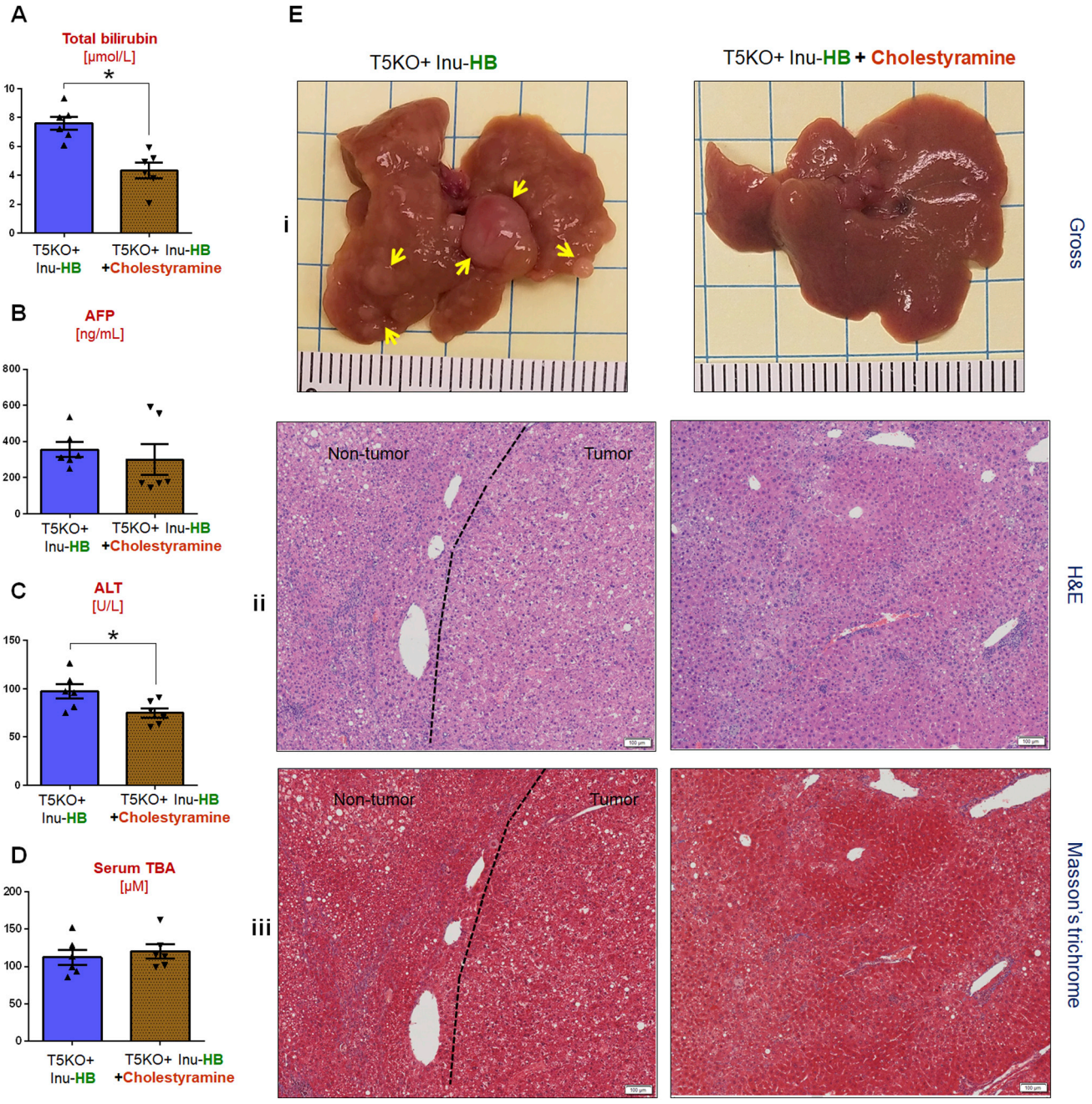

Figure S6. Cholestyramine Attenuate Inulin-Induced HCC, Related to Figure 6

ICD-fed male *Tlr5*KO mice were examined for serum bilirubin on day 15. All high bilirubin mice were then divided into two groups (n = 6 in each group); the first was continued on ICD, while the second was switched to ICD supplemented with cholestyramine (2% w/w). After 6 months, mice were euthanized and analyzed for HCC related parameters.

(A–D) Bar graphs represent serum level of (A) total bilirubin, (B) AFP, (C) ALT, and (D) total bile acid (TBA).

(E) (i) Macroscopic images of the liver. Arrowheads denote the tumors in ICD-fed mice, which are absent in ICD+cholestyramine-fed mice. (ii-iii) Representative image of (ii) H&E stained and (iii) Masson's trichrome stained liver sections (scale bar = 100 μm). The dotted line demarcates the tumor and non-tumor region. Data are expressed as Mean ± SEM (*$p < 0.05$).

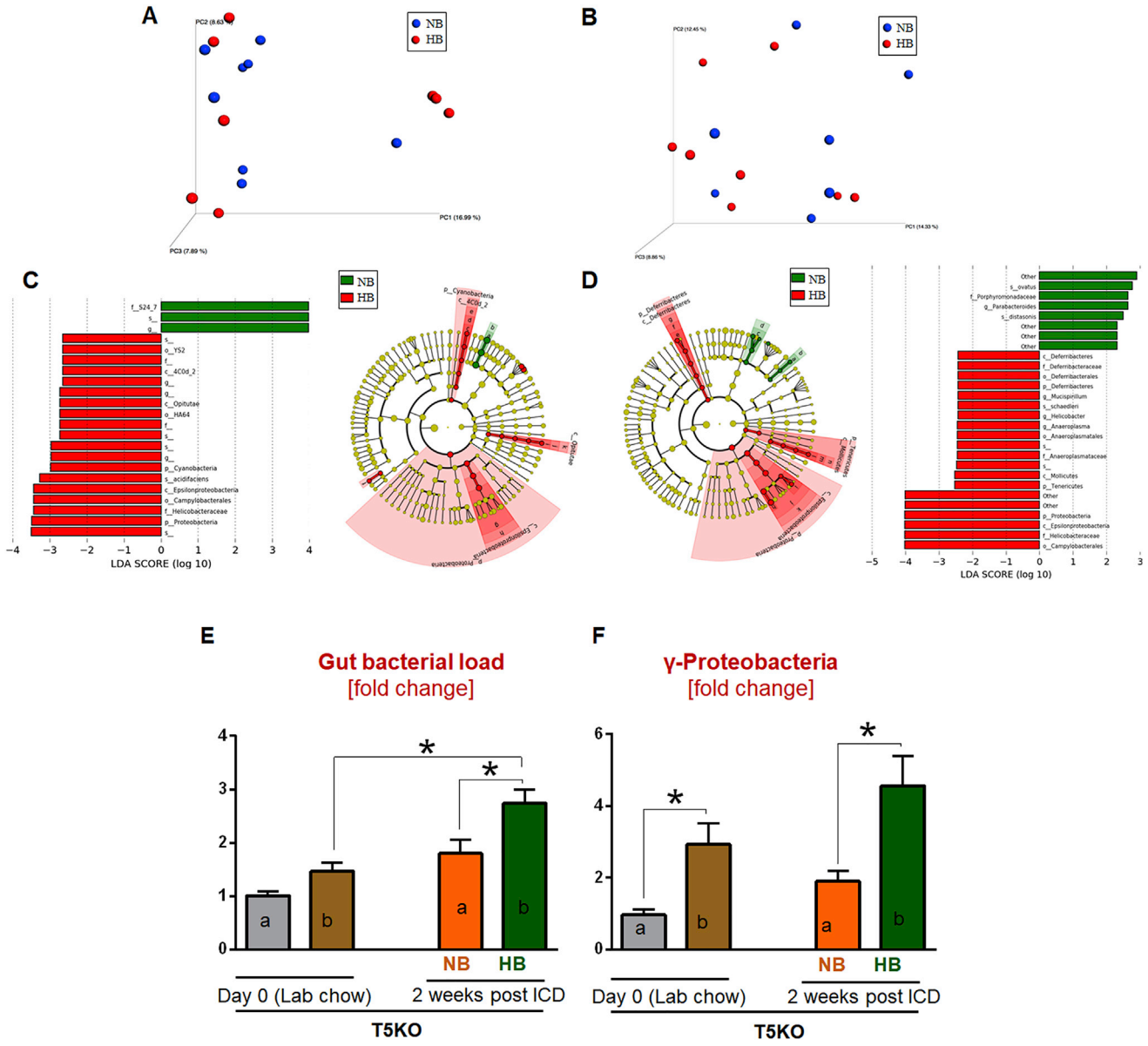

Figure S7. HCC-Susceptible Mice Exhibit Alterations in Gut Microbiota Characterized by an Increased Bacterial Load and Enrichment of *Proteobacteria* Even Prior to Dietary Intervention, Related to Figure 7

Fecal samples were collected from sixteen (male, 4 weeks old) *T5*KO mice before switching them to ICD. Subsequently, mice were fed ICD for 2 weeks and monitored for development of hyperbilirubinemia. Microbiota composition was analyzed in initial fecal material (day 0, prior to ICD feeding), and samples were retrospectively assigned to NB or HB group.

(A and B) Principal coordinate analysis of the unweighted Unifrac distance of initial (before dietary intervention) fecal microbiota, with samples colored based on NB or HB status. Results from two independent experiments are represented in A and B.

(C and D) LEfSE (LDA Effect Size) was used to investigate bacterial community that drives differences between NB and HB groups. Results from two independent experiments are represented in C and D.

(E and F) Bar graphs represent the fold change in total bacteria (E) and γ-proteobacteria (F) in *T5*KO mice; a and b denotes same group of mice analyzed at day 0 and post 2 weeks of ICD feeding.